Journal of Applied Polymer Science

# Effects of Surfactants on the Microstructures of Electrospun Polyacrylonitrile Nanofibers and Their Carbonized Analogs

**Yakup Aykut,[1] Behnam Pourdeyhimi,[2] Saad A. Khan[3]**

[1]Department of Textile Engineering, Uludag University, Gorukle, Bursa, Turkey

[2]Fiber and Polymer Science, Department of Textile Engineering, Chemistry and Science, North Carolina State University, Raleigh, North Carolina 27695-8301

[3]Chemical and Biomolecular Engineering, North Carolina State University, Raleigh, North Carolina 27695-7905

Correspondence to: Yakup Aykut (E-mail: aykut@uludag.edu.tr)

**ABSTRACT:** In this study, the influence of surfactants on the processability of electrospun polyacrylonitrile (PAN) nanofibers and their carbonized analogs was investigated. The surfactants employed in this effort are Triton X-100 (nonionic surfactant, SF-N), sodium dodecyl sulfate (SDS) (anionic surfactant, SF-A), and hexadecyltrimethylammonium bromide (HDTMAB) (cationic surfactant, SF-C). Interactions between electrospun PAN and the surfactants, reflected in effects on as-spun and carbonized nanofiber morphologies and microstructures, were explored. The results show that uniform nanofibers are obtained when cationic and anionic surfactants (surfactant free and nonionic surfactants) are utilized in the preparation of electrospun PAN. In contrast, a bead-on-a-string morphology results when the aniconic and cationic surfactants are present, and defect structure is enhanced with cationic surfactant addition. Moreover, fiber breakage is observed when the nonionic surfactant Triton X-100 is employed for electrospinning. After carbonizaition, the PAN polymers were observed to have less ordered structures with addition of any type of surfactant used for electrospinning and the disorder becomes more pronounced when the anionic surfactant is utilized. Owing to the fact that microstructure defects create midband gap states that enable more electrons to be emitted from the fiber, an enhancement of electron emission is observed for PAN electrospun in the presence of the anionic surfactant. © 2013 Wiley Periodicals, Inc. J. Appl. Polym. Sci. 000: 000–000, 2013

**KEYWORDS:** electrospinning; nanostructured polymers; morphology

Received 26 February 2013; accepted 3 June 2013; Published online
**DOI: 10.1002/app.39637**

## INTRODUCTION

Nanostructured materials have been produced using a variety of different substances including polymers, ceramics, metals, composites, and hybrid materials.[1–4] Using these nanostructured materials in devices typically leads to enhanced performances compared to cases where micro- and macroscale analogs are employed. Moreover, the patterns and shapes of nanomaterials can have an important impact on the performances of devices. In this regard, carbon nanostructured materials possess properties that are highly promising for many applications including electrode materials in energy devices (battery anodes), electron emission sources, oil spill remediation agents, and reinforcement materials for composites.[5–8] Among other properties, their field emission characteristics make carbon nanostructured materials particularly attractive for use as electron sources in devices such as field emission displays (FEDs), cold cathodes, electron microscopes, microwave generators, and field effect transistors (FETs).[9–13]

Carbon-based materials, in the forms of nanofilms (graphenes and graphite layers), nanoparticles (fullerenes: $C_{60-100}$), and nanotubes (CNTs), have been produced by using a number of different precursors and techniques.[14–16] Compared with nanofilm forms composed of nanoparticles and layered films, carbon in a one dimensional (1D) nanofiber form, has advantageous features because the high aspect ratio of carbon leads to an large increase in the total surface area.[17] 1D carbon nanostructures have been generated previously by using a variety of different precursors and techniques, including electrospinning, laser ablation, arc discharge, plasma-enhanced chemical vapor deposition, solid-state pyrolysis, ball milling, and high-pressure carbon monoxide deposition (HiPco).[18–24] Electrospinning is a novel technology that enables the production of continuous carbon nanofibers in the form of nonwoven webs from a variety of polymeric materials, including polyacrylonitrile (PAN),[29] Polybenzimidazol (PBI),[30] polyvinylalcohol (PVA),[31] polyimides,[32] and polymer

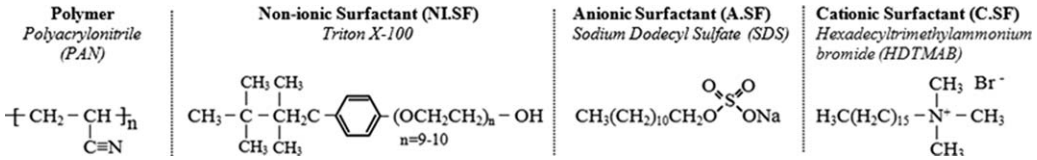


**Figure 1.** Chemical structures of the polymer, nonionic, anionic, and cationic surfactants.

blends.[33] In the process, a polymer solution is prepared and electrospun giving the as-spun polymer nanofibers that are properly stabilized in air and then carbonized in an inert atmosphere at elevated temperatures to form carbon nanofibers.

Surfactants play an important role in the fabrication of carbon-based materials, because they facilitate processability of carbon precursors and can be employed to alter in a controlled manner the properties of carbon. Various attempts have been made to use ionic surfactants in the production of nanostructured carbon. For example, coaxial electrospinning of PAN in the presence of Triton X-100 was examined by Yu et al. These workers observed that diameters of the polymeric fibers can be changed by altering the concentration of the surfactant in the sheath fluid.[25] The effect of the cationic surfactant dodecyltrimethylammonium bromide (DTBA) on the morphology of electrospun PAN nanofibers was investigated by Lin et al.[26] The observation made in that effort showed that the size and number of beads in the nanofiber mat as well as the average fiber diameter decrease upon addition of DTBA. In a study by Kurban et al., it was observed that 4-styrenesulphonic acid influences electrospinning of PAN by reducing bead formation at low solution viscosities.[27] In another study, Zheng et al. found that addition of cetyltrimethylammonium bromide ($C_{16}$TAB) leads to an increase in the dispersion of Pt nanoparticles on nanoporous carbon and that the surfactant promotes formation of microporous carbon independent of whether or not Pt particles are present.[28]

In the study described below, we investigated the effects of ionic and nonionic surfactants on the processing, final morphology, and material properties of electrospun PAN and the corresponding carbonized nanofibers (CNFs). In addition, we have determined the influences of the ionic surfactants on the field electron emission properties of the carbon nanofibers. The results show that electron emission from PAN, electrospun in the presence of the anionic surfactant sodium dodecyl sulfate (SDS), is enhanced.

## EXPERIMENTAL

### Materials and Electrospinning Process

The electrospinning stock solution containing 8 wt % of PAN (molecular weight of *ca.* 150,000 g $mol^{-1}$, Mw: 102.700 Mn: 60.600, Scientific Polymer Product, Ontario, NY, USA) was prepared by adding PAN to N,N-Dimethylformamide (DMF) in a vial followed by vigorous magnetic stirring at 70°C until a homogeneous solution was obtained. Each surfactant (0.05 g) was then added and the resulting solution was stirred for 1 h at ambient temperature. The solutions were kept under ambient conditions for 2 h before the electrospinning process. All surfactants, including Triton X-100 were the nonionic surfactant, SDS was the anionic surfactant, and hexadecyltrimethylammonium bromide (HDTMAB) was the cationic surfactant, were purchased from Sigma-Aldrich, Chemical. The electrospinning process for forming carbon nanofibers is schematically illustrated in Figure 2. After a proper electrospinning at an ambient condition, the as-spun PAN/SF nanofibers are stabilized in an air atmosphere at 280°C for 1 h and then carbonized in a nitrogen atmosphere at a heating rate of 5°C/min until 800°C for 2 h. The detail of electrospinning of carbon nanofibers from different precursors have been reported by different groups.[29–33]

### Characterization of Nanofibers

A solution parameters of the polymers were determined under ambient conditions. Viscosities of the solutions were measured with a TA Instrument AR-2000 Rheometer with a 2° cone and 40 mm diameter plate geometry. Conductivities of the solutions were measured with Fisher Scientific™'s Accumet™ Excel XL50 Conductivity Meter. All nanofiber morphologies were determined using field emission scanning electron microscopy (FEI/Philips XL30 SEM-FEG) with an acceleration voltage of 5 kV. All SEM samples were coated with gold at approximately 100°A thickness before imaging (DentonVacuum Desk IV sputter coater). ATR-FTIR (Thermo Scientific™) spectra of as-spun PAN/SF nanofibers were collected in the spectral range of 3500–750 $cm^{-1}$ and spectral resolution of 0.125 $cm^{-1}$. At least 124

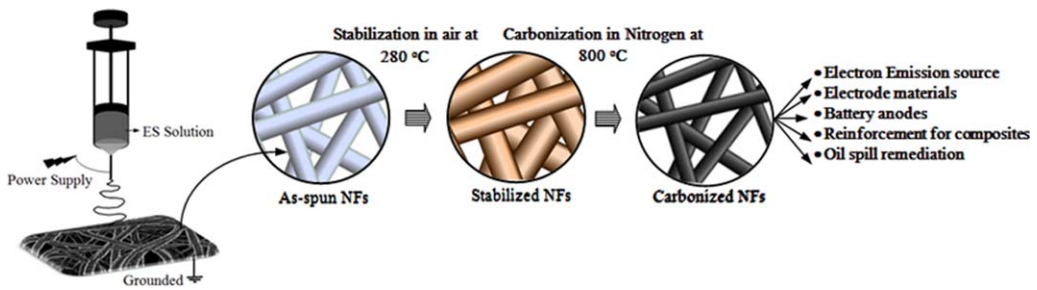


**Figure 2.** Schematic illustration of the electrospinning, stabilization, and carbonization processes. [Color figure can be viewed in the online issue, which is available at wileyonlinelibrary.com.]

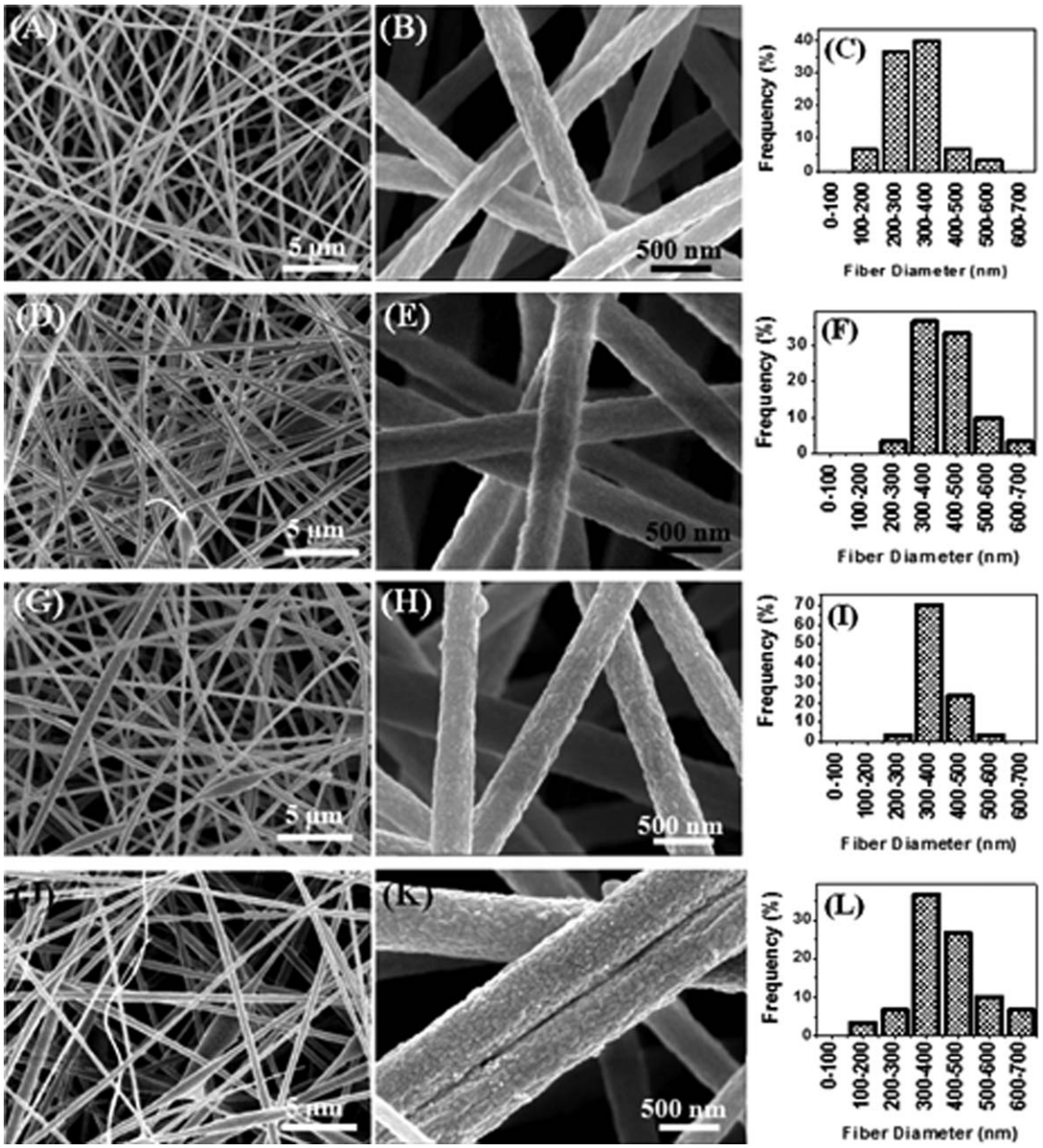


**Figure 3.** SEM images and diameter distribution of electrospun PAN/SF nanofibers with different surfactants: (A,B,C) pure PAN, (D,E,F) PAN/NI.SF, (G,H,I) PAN/A.SF, and (J,K,L) PAN/C.SF.

scans were collected to minimize the noise. Thermal analysis of PAN/SF nanofibers were conducted using a TA-Instruments Differential Scanning Calorimeter (DSCs – Q2000) in the temperature range of 100–350°C (heating rate of 10°C $min^{-1}$ under a nitrogen atmosphere). Weight losses of PAN/SF nanofibers in an air and nitrogen atmosphere were performed with a thermogravimetric analyzer (TA-Instruments TGA-Q500) by heating from 25 °C to 800°C (heating rate of 10°C $min^{-1}$). Raman spectra of the CNFs/SF were recorded with a Horiba Jobin Yvon LabRAM ARAMIS microscope with the laser line of 632 nm from a He–Ne excitation source. Electron field emissions (FE) of the CNFs/SF were measured with a scanning electron microscope (Hitachi S-3200) in vacuum by using the faraday cup method. The procedure used for this method was briefly explained in a previous publication.[34]

## RESULTS AND DISCUSSION

The morphologies of electrospun PAN and PAN/SF nanofibers were evaluated using the SEM technique. SEM images and fiber diameter distribution data are given in Figure 3(A–L). As seen by viewing the images, all NFs are randomly distributed and exhibit 3D nanofibrous web structures. The average fiber diameters of as-spun PAN, PAN/NI.SF, PAN/A.SF, and PAN/C.SF are 329, 437, 372, and 451 nm, respectively (Table I). The fiber diameters increase when each of the surfactants is present in the

**Table I.** Characteristic Properties of the Electrospinning Solutions and the Diameters of Electrospun PAN and Carbonized Nanofibers

| Samples | Viscosity (Pa s) | Surface tension (dyn/cm) | Conductivity (μs/cm) | PAN-diamater[a] (nm) | Stb-diameter[b] (nm) | CNFs-diamter[c] (nm) |
|---|---|---|---|---|---|---|
| PAN | 0.52 | 35.2 | 65.3 | 329 | 349 | 219 |
| PAN/NI.SF | 0.55 | 35.5 | 62.62 | 437 | 362 | 308 |
| PAN/A.SF | 0.49 | 34.5 | 993.6 | 372 | 341 | 266 |
| PAN/C.SF | 0.44 | 35.7 | 865.2 | 451 | 394 | 458 |

***Note.*** PAN, poly acrylonitrile; NI.SF, nonionic surfactant (Triton X-100); A.SF, anionic surfactant (SDS: Sodium Dodecyl Sulfate); C.SF, cationic surfactant (HDTMA, hexadecyltrimethylammonium bromide).

[a] Diameters of PAN nanofibers.

[b] Diameters of Stabilized nanofibers.

[c] Diameters of Carbonized nanofibers. The values of the surface tensions and nanofiber diameters were expressed as means ± standard deviations.

ES solution and a maximum average fiber diameter is observed when the cationic surfactant is included. In the electrospinning process, the fiber diameter is governed by complex set of chemical interactions taking place in the solution associated with viscosity, surface tension, and electrical conductivities.[35] As shown by viewing the data given in Table I, the surface tensions of the ES solutions do not change significantly upon addition of the surfactants. Consequently, the changes observed in the fiber diameters are related to both a change of solution electrical conductivity and viscosity. An increase of viscosity and decrease of conductivity leads to an increase of the average fiber diameter when the nonionic surfactant Triton X-100 is included, owing to the existence of hydrogen bonds between Triton X-100 and the CN groups of PAN and hydrophobic interaction between hydrophobic tails of this surfactant and carbon chains of PAN.[25] The average fiber diameter increases even though the viscosity decreases and electrical conductivity increases when both the anionic and cationic surfactants are present in the ES solution. This is a counter-intuitive finding because the average diameters of fibers in an electrospinning process usually increase with increasing solution viscosities and decrease with increasing solution electrical conductivities. As seen from viewing low magnification SEM images of the fiber samples (Figure 4), no defect structures are observed in the as-spun PAN sample [Figure 4(A)]. In contrast, bead defect structures are present in the fibers formed using the anionic and cationic surfactants containing ES solution [Figure 4(C,D)], and this defect is very high at cationic surfactant sample

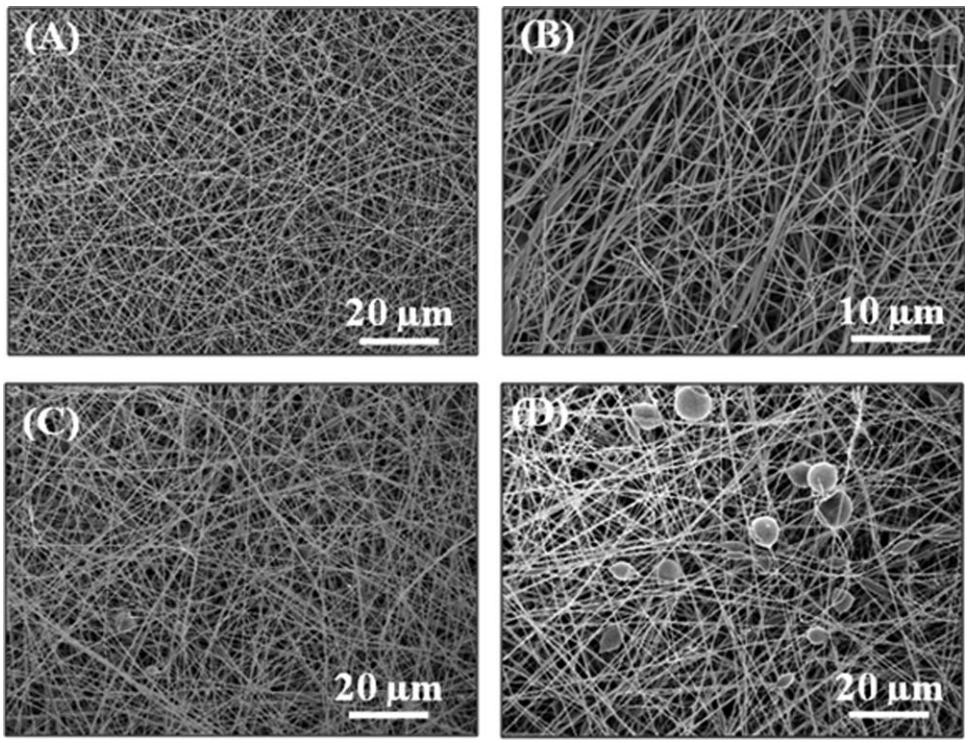


**Figure 4.** Low magnification SEM images and diameter distributions of electrospun PAN/SF nanofibers with different surfactants: (A) pure PAN, (B) PAN/NI.SF, (C) PAN/A.SF, and (D) PAN/C.SF.

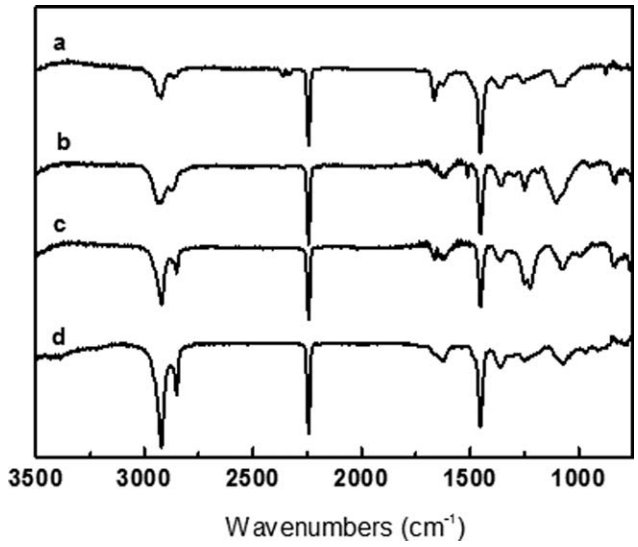


**Figure 5.** ATR-FTIR spectra of electrospun PAN/SF nanofibers with different surfactants: (a) pure PAN, (b) PAN/NI.SF, (c) PAN/A.SF, and (d) PAN/C.SF.

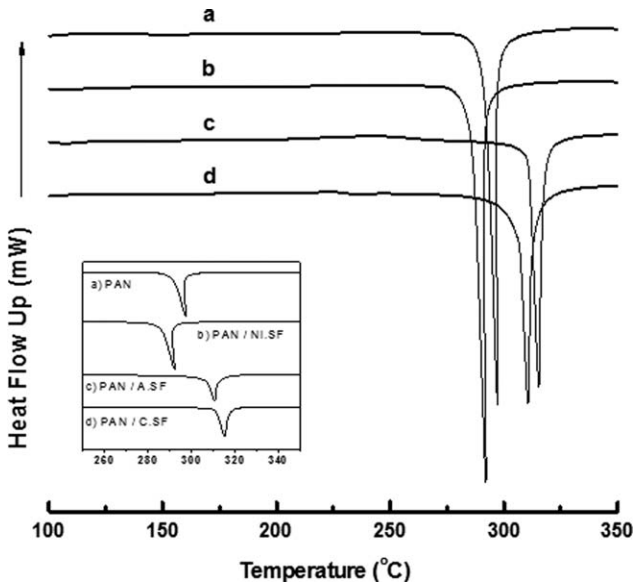


**Figure 6.** DSC thermograms of electrospun PAN/SF nanofibers with different surfactants: (a) pure PAN, (b) PAN/NI.SF, (c) PAN/A.SF, and (d) PAN/C.SF.

[Figure 4(D)]. This phenomenon is related to a decrease of solution viscosity with the addition of the cationic surfactant. In addition, breakage sites can be seen in the PAN NF fiber mat produced using the nonionic surfactant containing ES solution [Figure 4(B)].

ATR-FTIR spectra were recorded for each of the patterns and shapes fiber mat in the wavelength range 750–3500 $cm^{-1}$ in order to evaluate chemical interactions taking place in the as-spun pure and surfactant-assisted PAN nanofibers (Figure 5). The characteristics peaks of PAN occur at *ca.* 2921 and 2242 $cm^{-1}$ and are associated with stretching vibrations of the $CH_2$ (methylene) and C≡N (nitrile) groups.[36,37] Additionally, the bands associated with the surfactants are seen at *ca.* 1452, 2858, and 2921 $cm^{-1}$, corresponding to bending vibrations of $CH_2$, $-CH_3$ symmetric stretching modes, and the $CH_2$ stretching mode, respectively.[34,38] The peak at 1625 is assigned to the C=O vibration corresponding to residual DMF.[39] The characteristic FTIR bands of pure SDS at *ca.* 1083 and 1225 $cm^{-1}$ are ascribed to symmetric (vs S-O) and asymmetric (vs S-O) stretching of the sulfate group.[40] In the spectra, these bands appear at *ca.*1068 and 1218 $cm^{-1}$, wavelength changes that are related to electrostatic interactions taking place between the negatively charged SDS head groups and the nitrogens of the CN groups of PAN.[40] Stretching vibrations corresponding to the $C\text{-}N^+$ groups in HDTAMB are observed at *ca.* 910, 966, and 1108 $cm^{-1}$.[41]

The kinetics of reactions taking place during the stabilization process were determined by using DSC (Figure 6). When nanofibers are heated, the C≡N bonds in PAN are converted to C=N bonds and a ladder structure forms in the fibers.[42] The single sharp

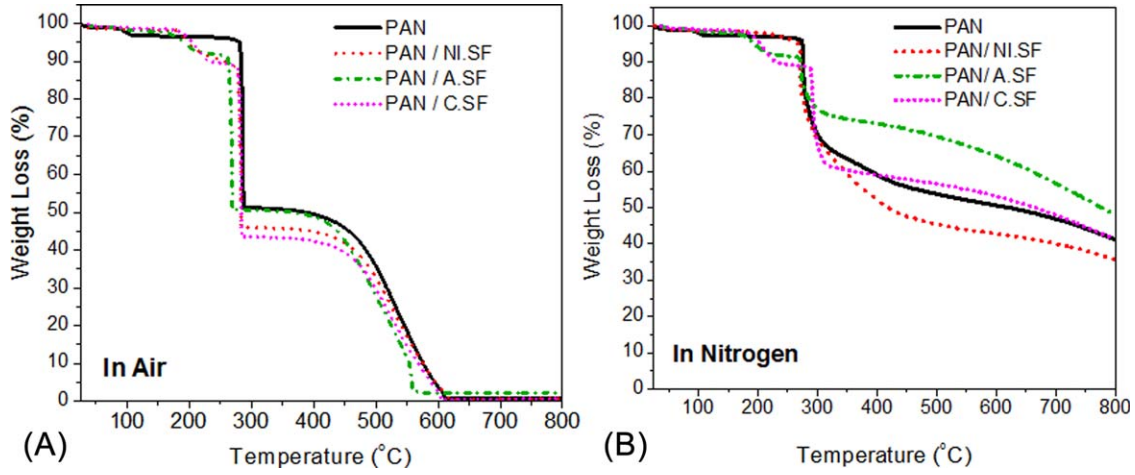


**Figure 7.** TGA thermograms of electrospun PAN/SF nanofibers with different surfactants: (A) in air atmosphere, and (B) in nitrogen atmosphere. [Color figure can be viewed in the online issue, which is available at wileyonlinelibrary.com.]

exothermic peak at *ca.* 298°C occurs in the DSC (Figure 6) that is associated with the main heat releasing reactions (dehydrogenation, cyclization, and crosslinking) taking place during the stabilization process.[43] This peak shifts to a higher temperature and broadens when the fiber is formed in the presence of SDS and HDTMAB. This observation suggests that the surfactants present in the nanofibers cause a reduction in the rate of free radical formation on the nitrile groups, which blocks their recombination reactions.[44] In contrast, the presence of Triton X-100 in PAN NFs lowers the temperature required for reaction, suggesting that formation of free radicals takes place readily and leads to an acceleration of the complex reactions occurring during stabilization.

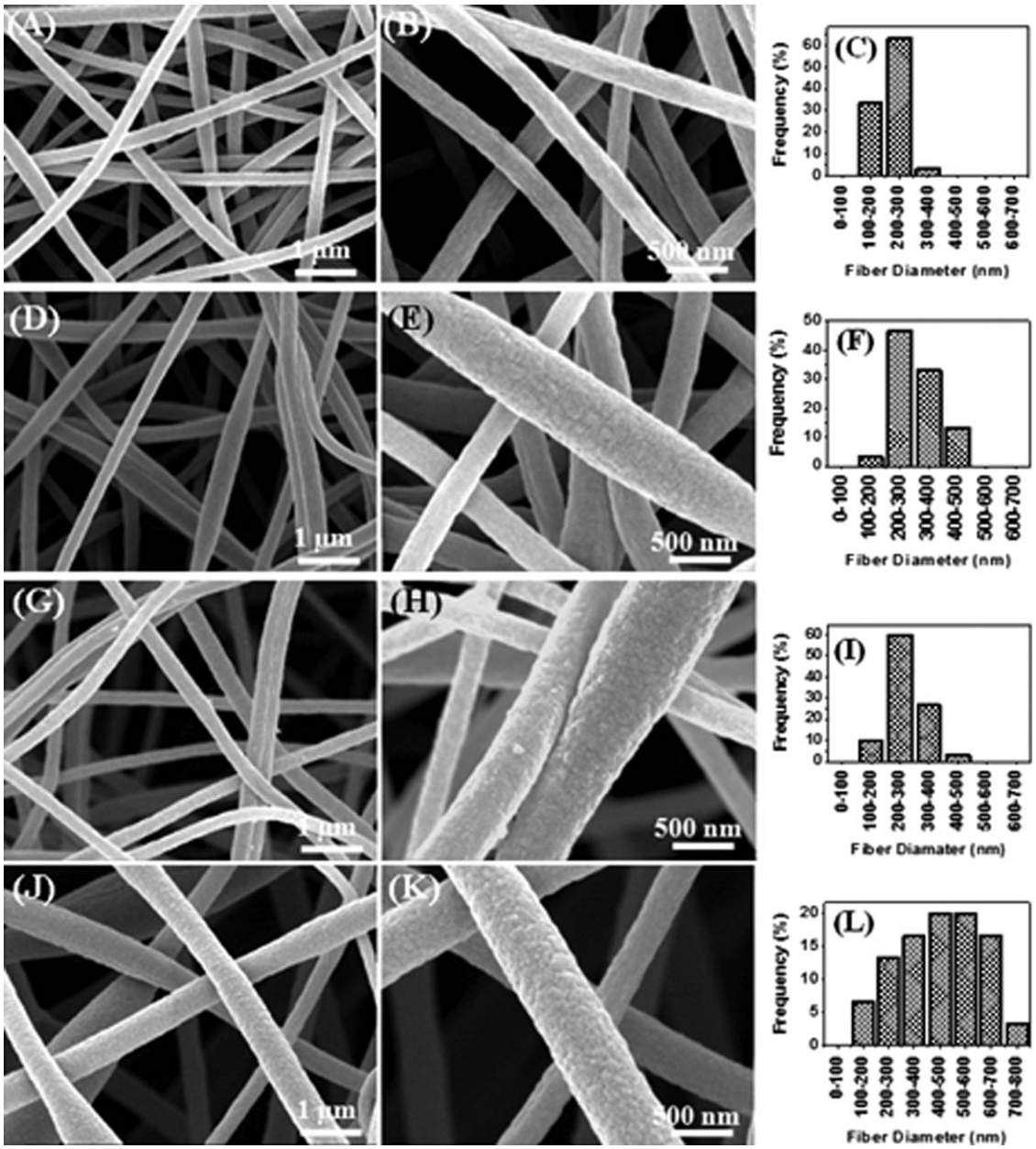


**Figure 8.** SEM images and diameter distributions of carbonized nanofibers with different surfactants: (A,B,C) pure CNFs, (D,E,F) CNFs/NI.SF, (G,H,I) CNFs/A.SF, and (J,K,L) CNFs/C.SF.

Thermal analyses of the fibers under air [Figure 7(A)] and nitrogen [Figure 7(B)] atmospheres were also carried out using a thermo gravimetric analyzer. The PAN NFs prepared in the presence of all of the surfactants in PAN begin decomposing at lower temperatures compared to that of pure PAN NFs [Figure 7(A)]. This observation suggests that the surfactants behave as dehydrogenation agents during stabilization of PAN. The initial rapid weight reduction taking place at *ca.* 100°C corresponds to the loss of water that is contained in the fibers. The abrupt weight loss that begins at *ca.* 278°C is associated with the main reactions (dehydrogenation, cyclization, and crosslinking) that occur in the PAN structure,[43] which take

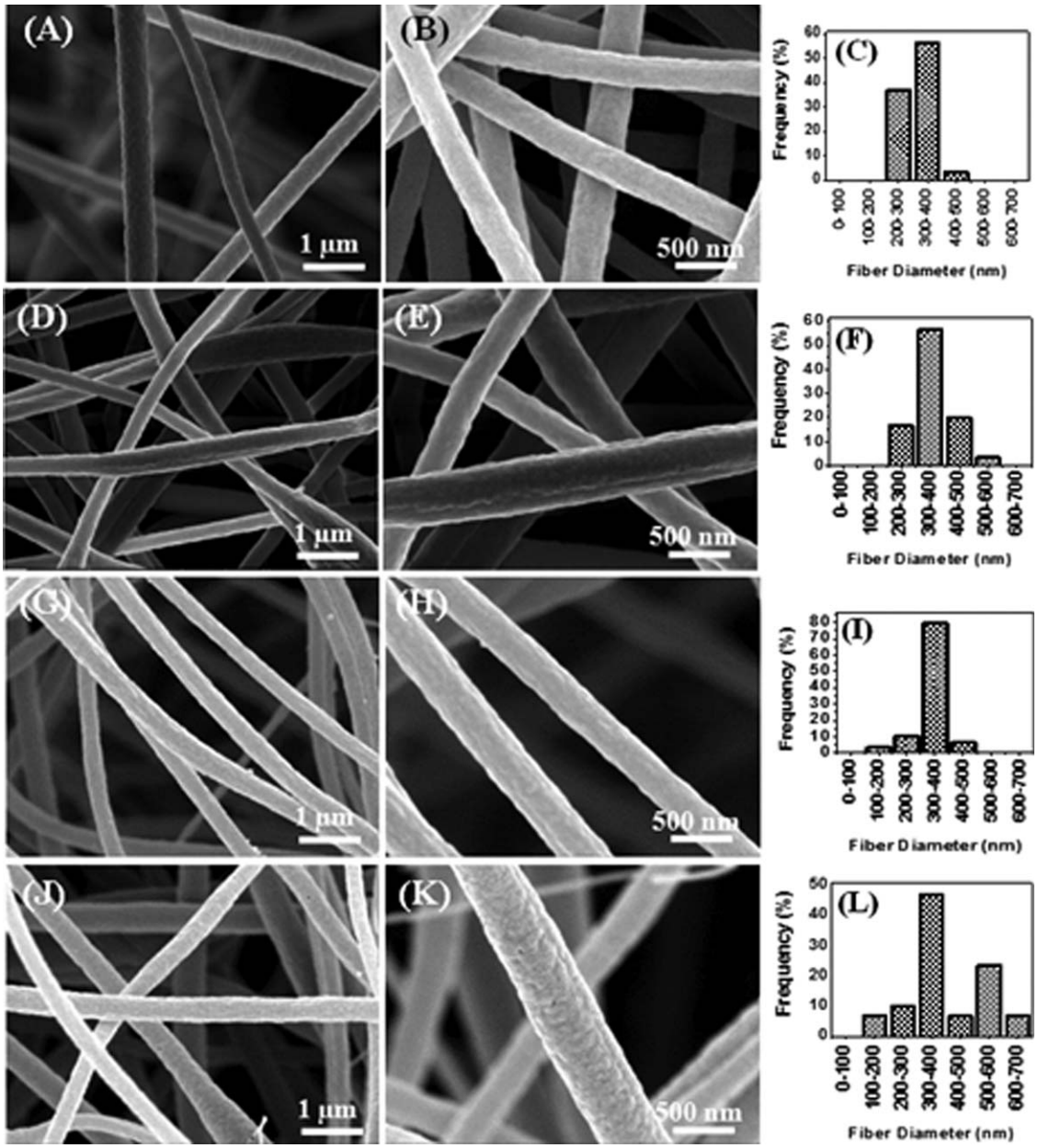


**Figure 9.** SEM images and diameter distributions of stabilized nanofibers with different surfactants: (A,B,C) pure stb-NFs, (D,E,F) stb-NFs/NI.SF, (G,H,I) stb-NFs /A.SF, and (J,K,L) stb-NFs /C.SF.

place in two steps starting at *ca.* 277°C (lose of volatiles) and extending to 432°C (combustional removal of volatiles).[45] The residues after TGA carried out in an air atmosphere are 0.8%, 0.72%, 2.09%, and 0.68% for pure PAN, PAN/NI.SF, PAN/A.SF, and PAN/C.SF NFs, respectively.

Weight losses associated with TGA under a nitrogen atmosphere mainly take place in the temperature range of 270–500°C. Decomposition of PAN samples formed from ES solutions containing surfactants begins at lower temperatures than that of pure PAN. These weight losses are caused by denitrogenation and the formation of the graphitic structures of the fibers. The observation that pure PAN and PAN/NI.SF nanofibers display only one sharp weight loss starting at temperatures in the range of 275–310°C can be attributed to a combination of the removal of volatiles and complex chemical reactions that occur during the stabilization process (dehydrogenation, cyclization, and crosslinking).[43] The weight loss starting temperature is higher for the PAN/C.SF sample (similar to the DSC results). The residues following TGA under a nitrogen atmosphere are 41.28%, 35.76%, 48.1%, and 41.42% for pure PAN, PAN/NI.SF, PAN/A.SF, and PAN/C.SF NFs, respectively.

SEM images of the CNFs along with diameter distribution data are given in Figure 8. As seen from viewing both Figure 8 and Table I, the average NF diameters of pure CNFs, CNFs/NI.SF, and CNFs/A.SF samples are vastly lower than those of their as-spun counterparts. The diameter reduction is perhaps caused by

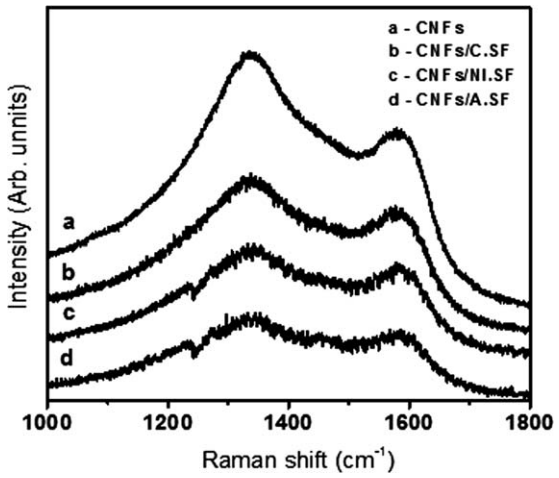


**Figure 10.** Raman spectra of carbonized nanofibers with different surfactants: (a) pure CNFs, (b) CNFs/NI.SF, (c) CNFs/A.SF, and (d) CNFs/C.SF.

the remove of chemical entities from the fiber and the formation of the dense graphitic carbon structure during the stabilization and final carbonization processes. Interestingly, the average nanofiber diameters of CNFs (CNFs/C.SF) derived from PAN NFs formed in the presence of surfactants are little higher than those of the as-spun PAN/C.SF counterpart. This phenomenon is likely the consequence of the fact that beads on the as-spun PAN/C.SF precursor nanofibers do not enable a large degree of fiber shrinkage during the carbonization process.

To further investigate the mechanism(s) of surfactant-assisted CNF formation, the morphologies of stabilized nanofibers were evaluated using SEM. As viewing of the images displayed in Figure 9 shows, surfaces of stabilized NFs are smoother than those of their as-spun and carbonized counterparts. Compared to those of as-spun NFs, the average NF diameters of all surfactant-assisted samples decrease after the stabilization process; a result of the loss of volatiles. Moreover, the fiber diameters are altered by the addition of each of the surfactants to the ES solution, a trend that parallels those of the as-spun and stabilized fibers and becomes more significant in the carbonized fibers.

The positions, bandwidths, and intensity ratios of Raman peaks provide important information about carbon structures. As a result, the structural features of the carbon nanofibers were investigated by using this spectroscopic method. Two characteristic Raman peaks for carbon are seen in the spectra (Figure 10) at *ca.* 1320 (D-band) and 1561 $cm^{-1}$ (G-band) that correspond to disordered carbons in the graphane layers and ordered graphite phases. The ratios of the intensities of these peaks ($R=I_D/I_G$) represent the degree of structurally ordered graphite phases present in the carbon nanofibers.[46,47] Inspection of the Raman spectra shows that the carbonized fibers have nearly the same peak intensity ratios (*ca.* 0.84) independent of whether or not surfactants were included in their preparation. However, the absolute values of the peak intensities decrease and their positions shift to longer wavelengths when surfactants are present. The peak intensity decreases are indicative of less ordered graphite structures in the carbon nanofibers, a phenomenon that is more dramatic for the anionic surfactant containing fiber. The surfactant induced decrease in the ordered structure of the carbon nanofibers is likely a consequence the carbonization of an additional organic substance that leads to a decrease in the percentage of carbonized PAN in total carbon structure. Also, the formation of product from decomposition of the sulfur containing group in the anionic surfactant can cause defects in the carbon nanofibers.[48]

In the final phase of this investigation, electron emission determinations were carried out on the nanofibers produced in this effort. The measurements, performed in ultrahigh vacuum chamber utilizing scanning electron microscopy and the Faraday cup method (see previous publication),[34] basically evaluate the number of secondary electrons that are emitted upon electron bombardment of the fibers. The results, given in current units in Table II, show that electron emission from the CNF, nonionic and anionic CNFs samples are approximately the same, but the number of electrons emitted from the anionic surfactant-assisted sample are considerably higher than those from the other samples. The latter finding appears to be associated with the presence of sulfur groups in the anionic surfactant, which leads to an increase in the defect density in the carbon structure that creates a continuum of energy levels within the band gap (mid gap) from which electron emission can take place.[48]

## CONCLUSIONS

In the study described above, we have explored the properties of several electrospun PAN nanofibers, which were prepared in the presence and absence of nonionic, cationic, and anionic surfactants. The effects of the surfactants on the morphological and microstructural properties of the as-spun nanofibers and their carbonized counterparts were probed. Possible carbonization mechanism with surfactant assisted can be determined by

**Table II.** Electron Emission Capacity from Surfactant-Assisted Carbon Nanofibers

| Samples | Beam current (A) | Absorbed current (A) | Emitted current (A) | Total electron emission coefficient (TEEC) |
|---|---|---|---|---|
| CNFs | 3.11E-10 | 2.65E-10 | 4.60E-11 | 0.147 |
| CNFs/NI.SF | 3.02E-10 | 2.58E-10 | 4.40E-11 | 0.145 |
| CNFs/C.SF | 2.88E-10 | 2.47E-10 | 4.18E-11 | 0.144 |
| CNFs/AI.SF | 2.95E-10 | 2.40E-10 | 5.50E-11 | 0.186 |

***Note.*** Five replicas were performed for each measurement and their averages were taken. The values of TEEC were expressed with means± standard deviations.

performing FTIR and NMR (1H and 13C) on the nanofibers at varying stages of the temperature treatment. Because, the addition of surfactant alters the properties of the ES solution (*eg.*, viscosity, surface tension, and conductivity), it should affect the morphologies of the as-spun fibers. The results demonstrate that all of the nanofibers are generated in the form of 3D nonofibrous mats, with those produced in a surfactant free and anionic surfactant included manner being highly uniform. In contrast, fiber breakage is observed when the nonionic surfactant is included in the ES solution and a bead-on-a-string structure is seen in the case of the cationic surfactant sample. The presence of all surfactants promotes formation of less disordered structures after carbonization, a phenomenon that is more obvious with the anionic surfactant sample. The latter defect creates a midband gap state that causes an enhancement of electron emission from the carbon fiber prepared using the anionic surfactant.

## ACKNOWLEDGMENTS

This study was supported by a grant from the Nonwovens Institute, NCSU, US and the Ministry of National Education, Republic of Turkey.

## REFERENCES

1. Aykut, Y. *J. Phys. Chem. Solids* **2013**, *74*, 328.
2. Aykut, Y.; Saquing, C.; Pourdeyhimi, B.; Parsons, G. N.; Khan, S. A. *Appl. Mater. Interfaces* **2012**, *4*, 3837.
3. Wu, H.; Hu, L.; Rowell, M. W.; Kong, D.; Cha, J.J.; McDonough, J.R.; Zhu, J.; Yang, Y.; McGehee, M.D.; Cui, Y. *Nano Lett.* **2010**, *10*, 4242.
4. Sahay, R.; Kumar, P. S.; Sridhar, R.; Sundaramurthy, J.; Venugopal, J.; Mhaisalkar, S.G.; Ramakrishna, S. *J. Mater. Chem.* **2012**, *22*, 12953.
5. Ji, L.; Zhang, X. *Electrochem. Commun.* **2009**, *11*, 684.
6. Darbari, S.; Abdi, Y.; Mohajerzadeh, S.; Soleimani, E. A. *Carbon* **2010**, *48*, 2493.
7. Zhoa, M.Q.; Huang, J. Q., Zhnag, Q. Luo, W. L. Wei. F. *Appl. Clay Sci.* **2011**, *53*, 1.
8. Ma, W.; Liu, L.; Zhang, Z.; Yang, R.; Liu, G.; Zhang, T.; An, X.; Yi, X.; Ren, Y.; Niu, Z.; Li, J.; Dong, H.; Zhou, W., Ajayan, P. M.; Xie, S. *Nano Lett.* **2009**, *9*, 2855.
9. De Heer, W. A.; Chatelain, A.; Ugarte, D. *Science* **1995**, *270*, 1179.
10. De Jonge, N.; Lamy, Y.; Schoots, K.; Oosterkamp, T. H. *Nature* **2002**, *420*, 393.
11. Giubileo, F.; Di Bartolomeo, A.; Sarno, M.; Altavilla, C.; Santandrea, S.; Ciambelli, P.; Cucolo, A. M. *Carbon* **2012**, *50*, 163.
12. Martel, R.; Schmidt, T.; Shea, H. R.; Hertel, T.; Avouris, Ph. *Appl. Phys. Lett.* **1998**, *73*, 2447.
13. Heeres, E. C.; Oosterkamp, T. H.; Jonge, N. D. *Phys. Rev. Lett.* **2012**, *108*, 36804.
14. Dresselhaus, M. S.; Dresselhaus, G.; Eklund, P. C. *Science of Fullerenes and Carbon Nanotubes*; Academic Press: New York, **1996**.
15. Plate, D. L.; Hart, A. J.; Reddy, C. M.; Gschwend, P. *Environ. Sci. Technol.* **2009**, *43*, 8367.
16. Vaughan, O. *Nature Nanotechnol.* **2010**, *5*, 386.
17. Meng, C.; Liu, C.; Fan, S. *Adv. Mater.* **2010**, *22*, 535.
18. Patil, S. A.; Chigome, S.; Hagerhall, C.; Torto, N.; Gorton, L. *Bioresour. Technol.* **2013**, *132*, 121.
19. Li, N.; Ma, Y; Wang, B.; Huang, Y.; Wu, Y; Yang, X.; Chen, Y. *Carbon* **2011**, *49*, 5132.
20. Chang-Jian, S. K.; Ho, J. R.; John Cheng, J. W. *Opt. Laser Technol.* **2011**, *43*, 1371.
21. Kucukayan, G.; Ovali, R.; Ilday, S.; Baykal, B.; Yurdakul, H.; Turan, S.; Gulseren, O.; Bengu, E. *Carbon* **2011**, *49*, 508.
22. Yuge, R.; Miyawaki, J.; Ichihashi, T.; Kuroshima, S.; Yoshitake, T.; Ohkawa, T.; Aoki, Y.; Lijima, S.; Yudasaka, M. *ACS Nano* **2010**, *4*, 7337.
23. Pierard, N.; Fonseca, A.; Konya, Z.; Willems, I.; VanTendeloo, G.; Nagy, J. B. *Chem. Phys. Lett.* **2001**, *335*, 1.
24. Georgakilas, V.; Voulgaris, D.; Vazquez, E.; Prato, M.; Guldi, D. M.; Kukovecz, A.; Kuzman, H. *J. Am. Chem. Soc.* **2002**, *124*, 14318.
25. Yu, D. G.; Chatterton, N. P.; Yang, J. H.; Wang, X.; Liao, Y. Z.; *Macromol. Mater. Eng.* **2012**, *297*, 395.
26. Lin, T.; Wang, H.; Wang, H.; Wang, X. *J. Mater. Sci. Technol.* **2005**, *21*, 1.
27. Kurban, Z.; Lovell, A.; Jenkins, D.; Bennington, S.; Loader, I.; Schober, A.; Skipper, N. *Eur. Polym. J.* **2010**, *46*, 1194.
28. Zheng, T.; Nishiyama, N.; Egashira, Y.; Ueyama, K. *Colloids Surf. A Physicochem. Eng. Asp.* **2005**, *262*, 52.
29. Yang, K. S.; Kim, C.; Park, S. H.; Kim, J. H.; Lee, W. J. *J. Biomed. Nanotechnol.* **2006**, *2*, 103.
30. Fatema, U. K.; Uddin, A. J.; Uemura, K.; Gotoh, Y. *Text. Res. J.* **2010**, *81*, 659.
31. Chung, G. S.; Jo, S. M.; Kim, B. C. *J. Appl. Polym. Sci.* **2005**, *97*, 165.
32. Kim, C.; Park, S. H.; Lee, W. J.; Yang, K. S. *Electrochim. Acta* **2004**, *50*, 877.
33. Kim, C.; Cho, Y. J.; Yun, W. Y.; Ngoc, B. T. N; Yang, K. S.; Chang, D. R.; Lee, J. W.; Kojima, M.; Kim, Y. A.; Endo, M. *Solid State Commun.* **2007**, *142*, 20.
34. Aykut, Y. *Appl. Mater. Interfaces* **2012**, *4*, 3405.
35. Son, W. K.; Youk, J. H.; Lee, T. S.; Park, W. H. *Polymer* **2004**, *45*, 2959.
36. Yuan, H.; Wang, Y.; Liu, P.; Yu, H.; Ge, B.; Mei, Y. *J. Appl. Polym. Sci.* **2011**, *122*, 90.
37. Ko, T. H.; Chen, C. Y. *J. Appl. Polym. Sci.* **1999**, *74*, 1745.
38. Kang, Y. H.; Ahn, K.; Jeong, S. Y.; Bae, J. S.; Jin, J. S.; Kim, H. G.; Hong, S. W.; Cho, C. R. *Thin Solid Films* **2011**, *519*, 7090.
39. Ji, L.; Medford, A. J.; Zhang, X. *J. Mater. Chem.* **2009**, *19*, 5593.

40. Yu, D. G.; Gao, L. D.; White, K.; White, C. B.; Lu, W. Y.; Zhu, L. M. *Pharm. Res.* **2010**, *27*, 2466.

41. Tunc, S.; Duman, O.; Cetinkaya, A. *Colloids Surf. A: Physicochem. Eng. Asp.* **2011**, *377*, 123.

42. Chen, H.; Wang, C. C.; Chen, C. Y. *Carbon* **2010**, *48*, 604.

43. Zhu, D.; Koganemaru, A.; Xu, C.; Shen, Q.; Li, S.; Matsuo, M. *J. Appl. Polym. Sci.* **2003**, *87*, 2063.

44. Ji, L.; Saquing, C.; Khan, A. S.; Zhang, X. *Nanotechnology* **2008**, *19*, 85605.

45. Kim, C.; Park, S. H.; Cho, J. I.; Lee, D. Y.; Park, T. J.; Lee, W. J.; Yang, K. S. *J. Raman Spectrosc.* **2004**, *35*, 928.

46. Rahman, M. M.; Jamal, A.; Khan, S. B.; Faisal, M. *J. Phys. Chem. C* **2011**, *115*, 9503.

47. Kim, C.; Yang, K. S.; Kojima, M.; Yoshida, K.; Kim, Y. J.; Kim, Y. A.; Endo, M. *Adv. Funct. Mater.* **2006**, *16*, 2393.

48. Gupta, S.; Weiss, B. L.; Weiner, B. R.; Morell, G. *Appl. Phys. Lett.* **2001**, *79*, 3446.